

## **AIMP1/p43 Negatively Regulates Adipogenesis by Inhibiting Peroxisome Proliferator-Activated Receptor Gamma**

Jong Hyun Kim<sup>1</sup>, Jung Ho Lee<sup>2</sup>, Min Chul Park<sup>1</sup>, Ina Yoon<sup>1</sup>, Kibom Kim<sup>1</sup>, Minji Lee<sup>5</sup>, Heung-Sik Choi<sup>3</sup>, Sunghoon Kim<sup>1,2,4,\*</sup>, Jung Min Han<sup>5,6,\*</sup>

<sup>1</sup>Medicinal Bioconvergence Research Center, Seoul National University, Seoul 151-742, South Korea

<sup>2</sup>College of Pharmacy, Seoul National University, Seoul 151-742, South Korea

<sup>3</sup>National Creative Research Initiatives Center for Nuclear Receptor Signals, School of Biological Sciences and Technology, Chonnam National University, Gwangju 500-757, South Korea

<sup>4</sup>Department of Molecular Medicine and Biopharmaceutical Sciences, Seoul National University, Seoul 151-742, South Korea

<sup>5</sup>Department of Integrated OMICS for Biomedical Science, Yonsei University, Seoul 120-749, South Korea

<sup>6</sup>College of Pharmacy, Yonsei University, Incheon 406-840, South Korea

\*Authors for correspondence (sungkim@snu.ac.kr and jhan74@yonsei.ac.kr)

Running title: AIMP1 negatively regulates PPAR $\gamma$

## Summary

Adipogenesis is known to be controlled by the concerted actions of transcription factors and co-regulators. However, little is known about the regulation mechanism of transcription factors that control adipogenesis. In addition, the adipogenic roles of translational factors remain unclear. Here, we show that aminoacyl-tRNA synthetase-interacting multifunctional protein 1 (AIMP1), an auxiliary factor that is associated with a macromolecular tRNA synthetase complex, negatively regulates adipogenesis via a direct interaction with the DNA-binding domain of peroxisome proliferator-activated receptor  $\gamma$  (PPAR $\gamma$ ). AIMP1 expression increased during adipocyte differentiation. Adipogenesis was augmented in AIMP1-deficient cells, as compared with control cells. AIMP1 exhibited high affinity for active PPAR $\gamma$  and interacted with the DNA-binding domain of PPAR $\gamma$ , thereby inhibiting its transcriptional activity. Thus, AIMP1 appears to function as a novel inhibitor of PPAR $\gamma$  that regulates adipocyte differentiation by preventing the transcriptional activation of PPAR $\gamma$ .

## Introduction

Aminoacyl-tRNA synthetase (ARS) catalyzes the ligation of a specific amino acid to its cognate tRNA, using ATP, thereby ensuring faithful translation of the genetic code (Kim et al., 2011; Park et al., 2008). Aminoacyl-tRNA synthetase-interacting multifunctional protein 1 (AIMP1) has been identified as a non-enzymatic factor associated with the ARS complex, which consists of nine different enzymes (Cirakoglu et al., 1985; Mirande et al., 1982; Norcum, 1989) and three non-enzymatic factors (Lee et al., 2004; Quevillon and Mirande, 1996; Quevillon et al., 1997; Quevillon et al., 1999). AIMP1 regulates the catalytic reaction of arginyl-tRNA synthetase (RRS) as well as the stability of the ARS complex through protein-protein interaction (Park et al., 1999; Han et al., 2006). AIMP1 is associated with various physiological functions, including angiogenesis (Park, et al., 2002b), wound healing (Park et al., 2005), and autoimmunity (Han et al., 2007). It is also highly enriched in pancreatic  $\alpha$  cells, from which it is secreted to maintain glucose homeostasis (Park, et al., 2006).

Adipose tissue is one the most dynamic types of tissue in the body and is a critical exchange center for complex energy transactions (Galic et al., 2010; Haque and Garg, 2004; Rosen and Spiegelman, 2006). However, an imbalance between energy intake and expenditure leads to metabolic disorders (Méndez-Sánchez, et al., 2006; Kalra et al., 2002). Adipogenesis, the cell differentiation mechanism by which preadipocytes become adipocytes, entails complex processes and steps such as

commitment of preadipocytes, growth-arrest, clonal expansion, terminal differentiation, and maturation of adipocytes (Grimaldi, 2001; Ntambi and Young-Cheul, 2000). The terminal stages of adipogenic differentiation have been extensively studied using immortalized preadipocyte lines (Couture et al., 2009; Han, et al., 2012).

Adipogenesis is governed by a multifaceted transcriptional regulatory cascade. Three classes of transcription factors are known to influence adipogenesis directly. These include peroxisome proliferator-activated receptor gamma (PPAR $\gamma$ ), member of the CCAAT/enhancer-binding protein families (C/EBPs), and members of the basic helix-loop-helix family (ADD1/SREBP1c) (Rosen et al., 2000). PPAR $\gamma$  is a member of the nuclear-receptor family of ligand-activated transcription factors that is highly expressed in white adipose tissues, where it is required for adipocyte differentiation (Koppen and Kalkhoven, 2010; Tontonoz et al., 2008). Accumulating evidence has suggested that no factor is capable of guiding cells to differentiate into adipocytes in the absence of PPAR $\gamma$ , whereas forced expression of PPAR $\gamma$  is sufficient to induce differentiation of fibroblasts into adipocytes (Rosen et al., 1999; Tontonoz et al., 1994). PPAR $\gamma$  activates the promoter of the gene encoding C/EBP $\alpha$ , and vice versa, creating a positive-feedback loop. In addition, PPAR $\gamma$  and C/EBP $\alpha$  induce the expression of genes that are involved in insulin sensitivity, lipogenesis, and lipolysis (Lefterova et al., 2008).

The sirtuin SIRT2, inhibits PPAR $\gamma$  indirectly by reducing the levels of acetylation of forkhead box O1 (FOXO1). This leads to an increase in the nuclear localization of FOXO1, where it represses the transcription of the gene encoding PPAR $\gamma$  (Jing et al., 2007). Another sirtuin, SIRT1, impairs adipogenesis by directly acting as a PPAR $\gamma$  co-repressor (Picard et al., 2004). The nuclear co-repressor (NCoR) and silencing mediator of retinoid and thyroid hormone (SMRT) proteins have been identified as nuclear receptor corepressors controlling transcriptional activity of PPAR $\gamma$  (Cohen et al. 1998; Yu et al., 2005). NCoR and SMRT recruit a complex exhibiting histone deacetylase activity to repress transcription of target genes. In addition, NCoR and SMRT are recruited by other nuclear receptors and interact with nuclear receptor corepressors in a ligand-dependent manner (Cohen, 2006; Yu et al., 2005).

Although PPAR $\gamma$  is known as an important factor playing a role in the strict control of adipogenesis, little is known about the regulation of PPAR $\gamma$  activity through protein-protein interaction. In this study, we show the molecular mechanisms by which AIMP1 regulates adipocyte differentiation through the catalytic inhibition of PPAR $\gamma$ .

## Results

### Dynamic alteration of AIMP1 expression during the differentiation of 3T3-L1 preadipocytes

During adipocyte differentiation, the gene expression profile changes markedly. While the adipogenic role attributed to the white adipose tissue (WAT) is energy storage, protein synthesis is an energy-consuming process (Trayhurn and Beattie, 2001; Rosen et al. 2000). Here, we specifically investigated the changes in expression of genes encoding tRNA synthetases and their associated factors that are involved in protein synthesis during adipogenesis. While the expression of genes encoding adipogenic markers, such as lipoprotein lipase (LPL), RXR $\alpha$ , and sterol regulatory element-binding transcription factor 1 (SREBP1), was increased during the differentiation of 3T3-L1 cells, the expression of SIRT1 was decreased, as was the expression of genes encoding ten different tRNA synthetases, glutamyl-prolyl-tRNA synthetase (EPRS), methionyl-tRNA synthetase (MRS), isoleucyl-tRNA synthetase (IRS), valyl-tRNA synthesis (VRS), tryptophanyl-tRNA synthetase (WRS), aspartyl-tRNA synthetase (DRS), arginyl-tRNA synthetase (RRS), leucyl-tRNA synthetase (LRS), glycyl-tRNA synthetase (GRS), and histidyl-tRNA synthetase (HRS), and that of genes encoding two AIMPs, AIMP2 and AIMP3 (Fig. 1A). These findings suggest that aminoacyl-tRNA synthesis and ATP consumption is decreased during adipogenesis. However, the expression pattern of the gene encoding AIMP1 was different from that of genes encoding AIMP2 and AIMP3.

AIMP1 expression peaked at 4-6 days after differentiation (Fig. 1A and 1B). While the protein expression of AIMP1 was slightly delayed, peaking only at 6-8 days after differentiation, the expression of RRS, which is a binding partner of AIMP1 within the multi-tRNA synthetase complex, remained unchanged during adipocyte differentiation (Fig. 1C). In addition, we also examined AIMP1 expression during adipose tissue development in mice. RT-PCR analysis was performed on RNA isolated from the developing WAT fractions at pre- and postnatal time points (Birsoy et al., 2011). As shown in Fig. 1D, AIMP1 mRNA was expressed relatively low in early embryonic (E15.5 and E16.5) and postnatal time points (P2 and P4), but its expression was greatly increased at E18.5 and P0 (Fig. 1D), consistent with AIMP1 expression in 3T3-L1 cells (Fig. 1B). Taken together, these results suggested that the stoichiometry of AIMP1 to RRS is altered and that AIMP1 has a novel function during adipocyte differentiation.

### **Nuclear localization of AIMP1 during adipogenesis**

To examine the function of AIMP1 during adipocyte differentiation, we first analyzed the subcellular localization of AIMP1. As shown in Fig. 2A, a portion of AIMP1 was clearly localized to the nucleus in differentiated 3T3-L1 adipocytes, but not in preadipocytes. Although AIMP1 was mainly expressed in the cytoplasm in 3T3-L1 preadipocytes, AIMP1 level was increased and translocated to the nucleus in mature adipocyte, where it colocalized with propidium iodide (PI) staining.

Biochemical fractionation also showed an increase in AIMP1 in both the cytoplasm and nucleus during adipogenesis (Fig. 2B).

To clarify the region of AIMP1 responsible for its nuclear translocation, we generated two truncated mutants of AIMP1 such as C-terminal truncated (amino acids [a.a.] 1-146) or N-terminal truncated mutant (a.a. 146-312). As shown in Fig. 2C, the N-terminal truncated mutant was mainly located in the nucleus while the C-terminal truncated mutant still showed cytoplasmic staining (Fig. 2C). To identify the residue of AIMP1 responsible for its nuclear translocation, we searched the candidate nuclear localization signal (NLS) of AIMP1 C-terminus using bioinformatics tools and found out one candidate NLS-triple lysine residues (<sup>267</sup>KKK<sup>269</sup>) of AIMP1 C-terminus (Fig. 2D). If these triple lysine residues are mutated to triple alanine residues, the mutated AIMP1 (KKK267-269AAA) cannot translocate to the nucleus (Fig. 2E). These results indicate that AIMP1 translocates to the nucleus via its NLS during adipocyte differentiation.

Since AIMP1 can function as a secreted factor (Park et al., 2002a; Park et al., 2005; Park et al., 2006; Han et al., 2010), we examined whether AIMP1 is secreted during adipogenesis. While adiponectin, an adipokine produced and secreted by adipocytes, was detected in the culture media of adipocytes, AIMP1 was not detected (Fig. 2F). Taken together, these results also suggested that AIMP1 has a novel function, in the nucleus, during adipogenesis.

## Negative regulation of adipogenesis by AIMP1

To investigate the effect of AIMP1 on adipogenesis, we used AIMP1-deficient mouse embryonic fibroblasts (MEFs) and 3T3-L1 preadipocytes that had been transfected with *AIMP1*-specific siRNA. The mRNA expression of adipogenic genes, such as those encoding acyl-CoA synthetase (ACS), fatty acid synthase (FAS), and SREBP-1, was elevated in AIMP1-deficient MEFs compared to that in wild type cells by 8 days after differentiation (Fig. 3A). The same results were observed in the *AIMP1* siRNA-transfected 3T3-L1 cells (Fig. 3B).

When the accumulation of intracellular lipids was monitored by Oil-red O staining, the intensity of Oil-red O staining was increased in AIMP1-deficient MEFs and in AIMP1 down-regulated cells (Fig. 3C and 3D). In addition, the triglyceride (TG) content was elevated in AIMP1-deficient MEFs and in AIMP1 down-regulated cells during adipogenesis (Fig. 3E and 3F). Expression of adipogenic proteins (aP2, RXR $\alpha$ , and C/EBP $\alpha$ ) rapidly increased in AIMP1-deficient MEFs and in AIMP1 down-regulated cells, as compared to control cells (Fig. 3G and 3H).

To examine whether AIMP1 overexpression suppresses adipogenesis, we generated cell lines with inducible *AIMP1*, which was overexpressed in the absence of tetracycline (tet). As shown in Fig. 4A, the expression of adipogenic markers, aP2 and C/EBP $\alpha$ , was decreased by induction of *AIMP1* expression during differentiation. Accumulation of intracellular lipid droplets and TG contents was suppressed in *AIMP1*-overexpressing cells, as shown by Oil-red O staining and TG

content assays (Fig. 4B and 4C). To examine the effect of the transient overexpression of *AIMP1* on adipogenesis, we generated an *AIMP1*-overexpressing adenovirus and infected it to 3T3-L1 preadipocytes. Expression of aP2 and C/EBP $\alpha$  was attenuated in cells infected with the *AIMP1*-adenovirus, compared with the control *LacZ*-adenovirus, during adipocyte differentiation (Fig. 4D). Furthermore, accumulation of intracellular lipid droplets and TG content was suppressed in cells infected with the *AIMP1*-adenovirus compared with the *LacZ*-adenovirus (Fig. 4E and 4F). Taken together, these results indicated that AIMP1 inhibits adipogenesis.

#### **Negative effect of AIMP1 on adipogenesis *in vivo***

To validate the effect of AIMP1 on adipogenesis *in vivo*, we injected the *LacZ*- or *AIMP1*-adenovirus into mouse epididymal fat pads. The epididymal fat pads (which are WAT), liver, and muscle tissues were removed from sacrificed mice and the expression of *AIMP1* and adipogenic markers was analyzed. When adenoviruses expressing either *AIMP1* or *LacZ* were injected into the fat pads, the expression of AIMP1 in the liver and muscle tissues was not affected (Fig. 5A). However, in the epididymal fat pads, expression of adipogenic marker proteins was changed significantly by *AIMP1*-adenovirus injection. Although the expression of lysyl-tRNA synthetase (KRS) was not changed by AIMP1 overexpression, the expression of FAS and aP2 was significantly reduced in *AIMP1*-adenovirus-injected epididymal fat pads compared to *LacZ*-adenovirus-injected epididymal fat pads (Fig. 5A, left

and right panel in WAT but not liver or muscle). Although the body weight of the mice and the plasma levels of AIMP1 were not changed by adenoviral infection of WAT, plasma TNF $\alpha$ , adiponectin, and TG contents were decreased in mice that had been infected with the *AIMP1*-adenovirus, as compared with those that had been infected with the *LacZ*-adenovirus (Fig. 5B-F). Conversely, both plasma non-esterified fatty acid (NEFA) and insulin levels were increased in mice infected with the *AIMP1*-adenovirus (Fig. 5G and 5H).

Next, we performed an i.p. glucose tolerance test (IPGTT) to compare the glucose sensitivity of *LacZ*-adenovirus-infected mice and *AIMP1*-adenovirus-infected mice. Overexpression of AIMP1 in WAT resulted in slower removal of blood glucose than did overexpression of LacZ in WAT (Fig. 5I). These results further indicated that AIMP1 is a negative regulator of adipogenesis *in vivo*.

### **Negative regulation of PPAR $\gamma$ by AIMP1**

To elucidate how AIMP1 regulates adipogenesis, we first examined the effect of AIMP1 on the transcriptional activities of PPAR $\gamma$ , SREBP1c, and ERR $\gamma$ , which are the major transcription factors involved in adipogenesis (Kim et al., 1998; Spiegelman 1998; Kubo et al., 2009). Although AIMP1 had no effect on the transcriptional activities of SREBP1c and ERR $\gamma$  (Supplementary materials Fig. 1A and 1B), AIMP1 suppressed PPAR $\gamma$  transcriptional activity in dose-dependent manner, as well as RXR $\alpha$ -induced PPAR $\gamma$  transcriptional activity (Fig. 6A and 6B).

Since AIMP1 mutant (KKK267-269AAA) cannot translocate to the nucleus (Fig. 2E), we investigated whether AIMP1 mutant (KKK267-269AAA) could regulate PPAR $\gamma$  transcriptional activity using luciferase assay in the absence or presence of rosiglitazone. AIMP1 mutant (KKK267-269AAA) did not suppress PPAR $\gamma$  transcriptional activity regardless of rosiglitazone while AIMP1 WT suppressed its transcriptional activity under the same condition (Supplementary materials Fig. 1C). These results suggest that nuclear translocation of AIMP1 is important for negative regulation of PPAR $\gamma$ .

Next, we investigated the association between PPAR $\gamma$  and AIMP1. Endogenous AIMP1 interacted with PPAR $\gamma$  in 3T3-L1 adipocytes (Fig. 6C). To assess whether AIMP1 binds specifically to particular isoforms of PPAR, we overexpressed either GFP-tagged PPAR $\gamma$  or PPAR $\delta$  in 293T cells that expressed myc-tagged AIMP1. AIMP1 co-immunoprecipitated with GFP-PPAR $\gamma$ , but not with GFP-PPAR $\delta$  (Fig. 6D). To identify the region of AIMP1 responsible for the interaction with PPAR $\gamma$ , several GFP-fusion constructs of PPAR $\gamma$  were generated. As shown in Fig. 6E, the full length PPAR $\gamma$  (a.a. 1-475) interacted with AIMP1. Although GFP-PPAR $\gamma$ -D (the DNA-binding domain; a.a. 94-181) as well as GFP-PPAR $\gamma$ -DL (the DNA-binding domain + the ligand-binding domain; a.a. 94-475) also interacted with AIMP1, GFP-PPAR $\gamma$ -L (the ligand-binding domain alone; a.a. 281-475) did not interact with AIMP1 under the same conditions. This finding indicated that the DNA-binding domain of PPAR $\gamma$  is required for interaction with AIMP1.

We then examined whether the conformation of PPAR $\gamma$  affects AIMP1 binding. Purified PPAR $\gamma$  was incubated with GST alone or GST-AIMP1 in the presence of GW9662 (a PPAR $\gamma$  antagonist) or rosiglitazone (a PPAR $\gamma$  agonist), followed by immunoblot analysis. Rosiglitazone, but not GW9662, significantly increased the binding affinity of PPAR $\gamma$  for AIMP1 (Fig. 6F). Since AIMP1 interacted with the DNA-binding domain of PPAR $\gamma$  and suppressed its transcriptional activity, we investigated whether AIMP1 directly inhibits the binding of PPAR $\gamma$  to the peroxisome proliferator-activated receptor response element (PPRE) on the DNA. Purified AIMP1 was incubated with nuclear extracts of differentiated 3T3-L1 cells and a biotin-labeled PPRE. As shown in Fig. 6G, purified AIMP1 prevented the binding of PPAR $\gamma$  to PPRE in a dose-dependent manner. Chromatin immunoprecipitation (ChIP) assays were performed to confirm the effect of AIMP1 on PPAR $\gamma$ -binding to target genes, such as those encoding aP2, LPL, and glycerol kinase (Gyk), in 3T3-L1 adipocytes. As shown in Fig. 6H, PPAR $\gamma$  dissociated from the promoter regions of the genes encoding aP2, LPL, and Gyk in 3T3-L1 adipocytes infected with the *AIMP1*-adenovirus. These results indicated that AIMP1 negatively regulates the transcriptional activity of PPAR $\gamma$  by competing with the PPAR $\gamma$  DNA-binding domain-target gene interaction.

## Discussion

AIMP1 plays distinct roles in specific cells and tissues. In our previous study,

we found that secreted AIMP1 functions in the maintenance of glucose homeostasis by inducing glucagon secretion in the pancreas, thus inhibiting glucose uptake and glycogenolysis in the liver, and enhancing lipolysis in adipose tissue (Park et al., 2006). Genetic depletion of AIMP1 induces hypoglycemia *in vivo* (Park et al., 2006). Here, we showed that, in adipose tissues, AIMP1 negatively regulates PPAR $\gamma$  and adipogenesis.

AIMP1 overexpression in WAT can affect blood levels of TNF $\alpha$ , insulin, adiponectin, NEFA, and TG. Thus, to some extent, the metabolic phenotypes of AIMP1<sup>-/-</sup> mice may be due to intracellular AIMP1 depletion and activation of PPAR $\gamma$  activity. Interestingly, liver PPAR $\gamma$  contributes to hepatic steatosis (Gavrilova et al., 2003; Yu et al., 2003), and AIMP1<sup>-/-</sup> mice show a hepatic steatosis phenotype (data not shown), which may be caused by hepatic elevation of PPAR $\gamma$  activity.

For adipocyte differentiation, cells first undergo growth-arrest, re-enter the cell cycle under the influence of differentiation inducers, undergo mitotic clonal expansion, and finally exit the cell cycle to undergo terminal differentiation (Gao et al., 2013; Tang et al., 2003). During the early phase of adipocyte differentiation, AIMP1 levels increase; the protein then translocates to the nucleus, where it interacts with and inhibits the transcriptional activity of PPAR $\gamma$  (Fig. 2B, Fig. 6A). As shown in Fig. 1A, the mRNA of *SIRT1*, a known repressor of PPAR $\gamma$ , was decreased during adipogenesis. Although *SIRT1* mRNA was decreased, PPAR $\gamma$  activity was not always high, indicating that other repressors are needed for the fine-

control of PPAR $\gamma$  activity during adipogenesis. Here, we suggest that AIMP1 is a novel inhibitor of PPAR $\gamma$  activity, and that the joint action of AIMP1 and SIRT1 in fine-tuning PPAR $\gamma$  activity may be required for control of adipogenesis.

Moreover, FOXO1 and SIRT2 are known to inhibit adipogenesis through PPAR $\gamma$  inhibition. Adipogenesis is regulated by acetylation/deacetylation of FOXO1, which is mediated by SIRT2. SIRT2 decreases the acetylation levels of FOXO1, which increases its binding to PPAR $\gamma$ , which, in turn, inhibits the transcriptional activity of PPAR $\gamma$  (Jing et al., 2007). FOXO1 also interacts with PPAR $\gamma$  in a rosiglitazone-dependent manner, but the regions responsible for binding of PPAR $\gamma$  to FOXO1 remain unclear (Wang and Tong, 2009). In this study, we showed that AIMP1 interacts with the DNA-binding domain of PPAR $\gamma$  in a rosiglitazone-dependent manner although the upstream regulator of AIMP1 remains unknown.

In this study, we revealed a novel role of AIMP1 in adipogenesis. Our data suggest that upon adipogenesis, AIMP1 is induced and translocated to the nucleus, where it binds to the DNA-binding domain of PPAR $\gamma$  and suppresses the transcription of the target gene mediated by PPAR $\gamma$ . This work identified a translational factor, AIMP1, as a new key player in the control of adipogenesis and suggests a potential connection between translation in cytosol and adipogenesis-related gene expression in nucleus. The physiological interaction between AIMP1 and PPAR $\gamma$  revealed here also provides a novel pharmacological space to deal with metabolic syndrome such as obesity.

## **Materials and Methods**

### **Quantitative RT-PCR (qPCR)**

Total RNA was isolated using TRIzol Reagent (Molecular Research Center, Cincinnati, OH, USA), according to the manufacturer's instructions. Total RNA was quantified by absorbance at 260 nm and the integrity of the RNA was checked using the 2100 Bioanalyzer (Agilent Technologies, Santa Clara, CA, USA). Target primer set sequences were acquired from the PrimerBank database or were designed using GenScript Real-time PCR primer design software (Supplementary Table. 1). RNA (1 µg) was reverse transcribed using a High Capacity cDNA Reverse Transcription Kit (Applied Biosystems, Foster City, CA, USA). qPCR was performed, in duplicate, using SYBR green (Qiagen, Hilden, Germany) and a Mx3000P (Agilent, Santa Clara, CA, USA). qPCR was performed using the following PCR cycling conditions: 95°C for 10 min, followed by 40 cycles each consisting of 95°C for 15 s, 55°C or 60°C for 30 s, and 72°C for 30 s. The relative abundance of specific mRNAs was calculated by normalization to the levels of the gene encoding glyceraldehyde-3-phosphate dehydrogenase.

### **Oil-red O staining and triglyceride measurement**

Oil-red O staining was performed as described previously (Wu et al., 1998). Medium was removed from differentiated cells; 10% formalin was added and cells were incubated for 5 min at RT. The formalin was replaced by new 10% formalin

and incubated for another 2 h at RT. Cells were washed well with 60% isopropanol and were incubated with oil-red O working solution (0.35% oil-red O in isopropanol: double-distilled water = 6:4, mixed immediately before use) for 10 min, which was then washed out with water. Triglyceride levels were measured using a Serum Triglyceride Determination Kit (Sigma-Aldrich, St Louis, MO, USA) according to the manufacturer's instructions.

### **Culture and differentiation of cells**

3T3-L1 and MEF cells were cultured in high-glucose (4500 mg/L) DMEM supplemented with 10% fetal bovine serum (DMEM medium). Differentiation of 3T3L1 preadipocytes was performed as described previously (Frost and Lane, 1985; Green and Kehinde, 1974; Zebisch et al., 2012). For 3T3-L1 adipocyte differentiation, cells were maintained for the indicated number of days post-confluency, and the medium changed to DMEM containing 0.25 mM IBMX (Wako Pure Chemical Industries), 1.0  $\mu$ M dexamethasone (Sigma-Aldrich, St Louis, MO, USA), and 5.0  $\mu$ g/ml human insulin (Sigma-Aldrich, St Louis, MO, USA) and were incubated for 2 days. The medium was then replaced by DMEM medium containing only 5.0  $\mu$ g/mL human insulin and the cells were maintained in this medium throughout adipocyte differentiation. For differentiation of 3T3-L1 cells that were to be used for electroporation, cells were differentiated at day 0 post-confluency, so that the effect of *AIMPI*-knockdown would last longer. The method used for

differentiation of MEFs was the same as that used for differentiation of 3T3-L1 cells, except that the culture medium was supplemented with 0.1  $\mu$ M rosiglitazone (Cayman) throughout differentiation.

### **Measurement of AIMP1 and adiponectin in the culture medium**

For the measurement of AIMP1 and adiponectin, cell culture medium was harvested at the indicated day, and clarified by centrifugation at 4000 x g for 15 min. The levels of AIMP1 and adiponectin in the medium were measured using ELISA kits according to the manufacturer's instructions.

### **Western blotting**

Cells were lysed with RIPA buffer (1% NP-40, 1% Na-deoxycholate, 0.1% SDS, 150 mM NaCl, 50 mM Tris pH 7.4, and 2 mM EDTA, 50 mM NaF) and incubated on ice for 30 min. The lysates were centrifuged for 20 min at 20,000 x g. Supernatants were quantified by BCA assay and boiled with 5 x Laemmli sample buffer. The samples were separated by SDS-PAGE and transferred to PVDF membrane. Proteins were detected using rabbit polyclonal AIMP1, PPAR $\gamma$  (sc-7273; Santa Cruz, Dallas, TX, USA), RXR $\alpha$  (sc-553; Santa Cruz, Dallas, TX, USA), C/EBP $\alpha$  (sc-61; Santa Cruz, Dallas, TX, USA), aP2 (sc-18661; Santa Cruz, Dallas, TX, USA), c-jun (sc-45-G; Santa Cruz, Dallas, TX, USA), c-fos (sc-52; Santa Cruz, Dallas, TX, USA),  $\gamma$ -tubulin (T6557, Sigma-Aldrich, St Louis, MO, USA), and GFP

(ab6556, Abcam, Cambridge, UK) antibodies.

### **Separation of stromal vascular fractions (SVF) and adipocyte fractions in mice**

Embryos and postnatal days 0, 2, 4 from C57BL/6 mice were minced in PBS with calcium chloride and 0.5% BSA. Tissue suspensions were centrifuged at 500g for 5 min to remove erythrocytes and free leukocytes. Collagenase type II (Gibco; Invitrogen, Carlsbad, CA, USA) was added to 1 mg/ml in DMEM and incubated at 37°C for 20 min with shaking. The cell suspensions were filtered through an 80 µm filter (BD bioscience, USA) and then spun at 300g for 5 min to separate floating adipocytes from the SVF pellet. To ensure proper isolation, adipocyte fractions were examined by microscopy before and after plating on plastic to detect adherent cells. Total RNA was isolated from cell by RNeasy kit (Qiagen, Hilden, Germany) (Birsoy et al., 2011).

### **RT-PCR**

RNA was extracted according to the protocols of the RNeasy kit (Qiagen, Hilden, Germany). RNA was reverse transcribed with M-MLV reverse transcriptase (Invitrogen, Carlsbad, CA, USA) and the cDNA was amplified by PCR and electrophoresed on ethidium bromide-agarose gels. Primers used for PCR were as follows: PPAR $\gamma$ -forward, 5'-CTGGTTTCATTAACCTTGATTTG-3', PPAR $\gamma$ -reverse, 5'-ACAAGTCCTTGTAGATCTCCTG-3', AIMP1-forward, 5'-CAG CAGTCGGCAGCAGCAAGTAC-3', AIMP1-reverse, 5'-CACACTCAGCATTGGT

GTGCAGG-3', GAPDH-forward, 5'-GTGAAGGTCGGTGTGAACGGA-3',  
GAPDH-reverse, 5'-CCCATCACAAACATGGGGGCA-3'.

### **Plasmids and transfection**

Mouse *AIMP1* cDNA was amplified from 3T3-L1 cells, digested with *EcoRI* and *SalI* enzymes, and cloned into a pcDNA3 vector (pcDNA3-mAIMP1). Human *AIMP1* was amplified with a myc-tag encoding primer and cloned into pcDNA3 vector (myc-AIMP1), and the native form of human *AIMP1* was amplified and cloned into a pGEX-4T1 vector (GST-AIMP1). pcDNA3-PPAR $\gamma$ 2, PPREx3TK-Luc, and GST-PPAR $\gamma$ 2 vectors were kindly provided by CS Shin (Seoul National University, Seoul, Korea) and the GFP-PPAR $\gamma$  vector was kindly provided by FJ Gonzalez (National Cancer Institute, USA). All transfection experiments were performed in the 3T3-L1 cell line, using electroporation (Neon, Invitrogen, Carlsbad, CA, USA) according to the manufacturer's protocol. Voltage, pulse width, and pulse number for electroporation were adjusted to 2500 V, 9 ms, and 1, respectively, for the 3T3-L1 cell line. For the *AIMP1* knockdown experiment, duplex RNAs were synthesized (Invitrogen; sequence: 5'-AACAATACAACCAATTCGAAGATCC-3') and transfected by electroporation as described above. Stealth<sup>TM</sup> RNAi Negative Control Duplexes (Invitrogen, Carlsbad, CA, USA) were used as control.

### **Site directed mutagenesis**

AIMP1 mutants were and generated by site-directed mutagenesis using manual methods. The mutants were confirmed by DNA sequencing. The following primers were used to generate it. AIMP1 (KKK267-269AAA)-Forward: 5'-TCA GGC TGG ATC TGC TCC CAA ATC GCC GCC GCA GGA TTC AGC TCC TTG TCA GGC TC-3', AIMP1 (KKK267-269AAA)-Reverse: 5'-GAG CCT GAC AAG GAG CTG AAT CCT GCG GCG GCG ATT TGG GAG CAG ATC CAG CCT GA-3'

### **Luciferase assay**

3T3-L1 cells were transfected with PPREx3TK-Luc, pcDNA3-PPAR $\gamma$ 2, and with increasing amounts of pcDNA3-mAIMP1. At 24 h after transfection, cells were lysed with Cell Culture Lysis Reagent (Promega, Madison, WI, USA), incubated for 30 min at 4°C and centrifuged for 1 min at 20,000 x g. Supernatants were transferred to a luminometer plate and luciferase activities were measured according to the manufacturer's protocol (LB96V MicroLumat Plus; EG&G). All experiments were performed in triplicate, and differences in transfection efficiency were compensated for by normalizing the luciferase activity to the  $\beta$ -galactosidase activity.

### **GST-pull down and immunoprecipitation**

GST, GST-AIMP1, and GST-PPAR $\gamma$ 2 proteins were purified as follows. Each vector was transformed into Rosetta cells and cultured in Luria broth (LB) media. Protein expression was induced by 0.5 mM IPTG, and cells were cultured at 18°C, for 9 h.

Cells were pelleted, resuspended in protein lysis buffer (50 mM Tris pH 7.4, 120 mM NaCl, 1 mM MgCl<sub>2</sub>, 1 mM CaCl<sub>2</sub>, 1 mM EDTA, 1% Triton X-100, and 100 µg/ml PMSF), and sonicated to disrupt cells. Cell lysates were centrifuged for 20 min at 20,000 x g; the supernatants were mixed with Glutathione Sepharose™ 4B (GE Healthcare, Little Chalfont, UK) beads and rotated for 6 h at 4°C in order to bind proteins to the beads. Differentiated 3T3-L1 cells were harvested in 0.1% NP-40 PBS buffer with 100 µg/mL PMSF and sonicated for two rounds of three pulses each, at 20% power output and a 50% duty cycle, using a Branson Sonifier 450. The 3T3-L1 lysates and protein-conjugated beads were mixed and the samples then rotated for 6 h at 4°C. Proteins were pelleted with the beads by centrifugation, and were then detected by western blotting. Immunoprecipitation of proteins obtained from transiently transfected cells was performed in the same way as the GST-pull down assay, except that IgG or myc antibodies (sc-40; Santa Cruz, Dallas, TX, USA) were conjugated to Protein G Agarose beads (Invitrogen, Carlsbad, CA, USA).

### **Electrophoretic mobility shift assay (EMSA)**

EMSA was performed using an EMSA “Gel-Shift” kit (Panomics, Fremont, CA, USA) according to the manufacturer’s protocol. Briefly, eluted GST, or GST-AIMP1 proteins were incubated with differentiated 3T3-L1 nuclear extracts, binding buffer, poly d(I-C), and a biotin-labeled PPRE probe, before being separated by SDS-PAGE. 3T3-L1 nuclear extract was prepared by disruption and centrifugation of 3T3-L1

cells in 0.5% NP-40 sucrose buffer. An unlabeled PPRE probe was used as the cold probe. Probe signals were detected by western blotting using a streptavidin-horseradish peroxidase conjugate.

### **Preparation of recombinant adenovirus**

Recombinant adenovirus containing human *AIMPI* cDNA was constructed using an Adenoviral Expression Kit (Clontech, Mountain View, CA, USA). Recombinant adenoviruses bearing the bacterial  $\beta$ -galactosidase gene (Adv-LacZ) was used as control.

### **Animals and *in vivo* adenovirus injection into the fat pad**

Animal studies were conducted in accordance with the institutional guidelines for animal experiments of Seoul National University. Male C57BL/6 mice were housed individually, and high-fat-chow feeding (32% safflower oil, 33.1% casein, 17.6% sucrose, and 5.6% cellulose) was initiated at 5 weeks of age. After 4 weeks of high-fat-chow loading, body-weight-matched mice were anesthetized prior to dissection of the skin and body wall. An adenoviral preparation ( $1 \times 10^8$  plaque-forming units in a volume of 20  $\mu$ L) was injected at two points on each side of the epididymal fat pad and the subcutaneous fat tissues in the flank, i.e., each mouse was injected at a total of four points (Yamada et al., 2006).

### **Blood analysis**

Blood AIMP1, serum insulin, adiponectin, TNF $\alpha$ , triglyceride, and NEFA levels were determined as previously described (Park et al., 2006).

### **Intraperitoneal glucose-tolerance test (IPGTT)**

IPGTTs were performed on fasted (10 h, daytime) mice. Mice were given glucose (2 g/kg of body weight) intraperitoneally, followed by measurement of blood glucose levels.

### **Acknowledgements**

This work was supported by the Global Frontier Project grant (NRF-M3A6A4-2010-0029785, NRF-M3A6A4072536), by the Basic Science Research Program (2012R1A1A2040060) of the National Research Foundation, funded by the Ministry of Science, ICT & Future Planning (MSIP) of Korea, and by the Yonsei University Global Specialization Project of 2014.

### **REFERENCES**

**Birsoy K., Berry R., Wang T., Ceyhan O., Tavazoie S., Friedman J. M., Rodeheffer M. S.** (2011). Analysis of gene networks in white adipose tissue development reveals a role for ETS2 in adipogenesis. *Development*. **138**, 4709-4719.

**Cirakoglu, B., Mirande, M., and Waller, J. P.** (1985). A model for the structural organization of aminoacyl-tRNA synthetases in mammalian cells. *FEBS Lett.* **183**, 185-190.

**Cohen, R. N.** (2006). Nuclear receptor corepressors and PPARgamma. *Nucl. Recept. Signal.* **4**,e003.

**Cohen, R. N., Wondisford, F. E., and Hollenberg, A. N.** (1998). Two separate NCoR (nuclear receptor co-repressor) interaction domains mediate co-repressor action on thyroid hormone response elements. *Mol Endocrinol.* **12**,1567-1581.

**Couture, J. P., Daviau, A., Fradette, J., and Blouin, R.** (2009). The mixed-lineage kinase DLK is a key regulator of 3T3-L1 adipocyte differentiation. *PLoS One.* **4**,e4743.

**Frost, S. C., and Lane, M. D.** (1985). Evidence for the involvement of vicinal sulfhydryl groups in insulin-activated hexose transport by 3T3-L1 adipocytes. *J. Biol. Chem.* **260**,2646-2652.

**Fujimori, K.** (2012). Prostaglandins as PPAR $\gamma$  modulators in adipogenesis. *PPAR Res.* **12**,527607.

**Galic, S., Oakhill, J. S., and Steinberg, G. R.** (2010). Adipose tissue as an endocrine organ. *Mol. Cell Endocrinol.* **316**,129-139.

**Gao, Y., Koppen, A., Rakhshandehroo, M., Tasdelen, I., van de Graaf, S. F., van Loosdregt, J., van Beekum, O., Hamers, N., van Leenen, D., Berkers, C. R., Berger, R., Holstege, F. C., Coffey, P. J., Brenkman, A. B., Ovaa, H., and**

**Kalkhoven, E.** (2013). Early adipogenesis is regulated through USP7-mediated deubiquitination of the histone acetyltransferase TIP60. *Nat. Commun.* **4**,2656.

**Gavrilova, O., Haluzik, M., Matsusue, K., Cutson, J. J., Johnson, L., Dietz, K. R., Nicol, C. J., Vinson, C., Gonzalez, F. J., and Reitman, M. L.** (2003). Liver peroxisome proliferator-activated receptor gamma contributes to hepatic steatosis, triglyceride clearance, and regulation of body fat mass. *J. Biol. Chem.* **278**,34268-34276.

**Green, H., and Kehinde, O.** (1974). Sublines of mouse 3T3 cells that accumulate lipid. *Cell* **1**,113-116.

**Grimaldi, P. A.** (2001). The roles of PPARs in adipocyte differentiation. *Prog Lipid Res.* **40**,269-281.

**Han, J. M., Lee, M. J., Park, S. G., Lee, S. H., Razin, E., Choi, E. C., Kim, S.** (2006). Hierarchical network between the components of the multi-tRNA synthetase complex: implications for complex formation. *J. Biol. Chem.* **281**,38663-38667.

**Han, J. M., Myung, H., and Kim, S.** (2010). Antitumor activity and pharmacokinetic properties of ARS-interacting multi-functional protein 1 (AIMP1/p43). *Cancer Lett.* **287**,157-164.

**Han, J. M., Park, S. G., Liu, B., Park, B. J., Kim, J. Y., Jin, C. H., Song, Y. W., Li, Z., and Kim, S.** (2007). Aminoacyl-tRNA synthetase-interacting multifunctional protein 1/p43 controls endoplasmic reticulum retention of heat shock protein gp96:

its pathological implications in lupus-like autoimmune diseases. *Am. J. Pathol.* **170**,2042-2054.

**Han, R., Kitlinska, J. B., Munday, W. R., Gallicano, G. I., and Zukowska, Z.** (2012). Stress hormone epinephrine enhances adipogenesis in murine embryonic stem cells by up-regulating the neuropeptide Y system. *PLoS One.* **7**,e36609.

**Haque, W. A., and Garg, A.** (2004). Adipocyte biology and adipocytokines. *Clin. Lab Med.* **24**,217-234.

**Jing, E., Gesta, S., and Kahn, C. R.** (2007). SIRT2 regulates adipocyte differentiation through FoxO1 acetylation/deacetylation. *Cell Metab.* **6**,105-114.

**Kalra, P. S., and Kalra, S. P.** (2002). Obesity and metabolic syndrome: long-term benefits of central leptin gene therapy. *Drugs Today (Barc)* **38**,745-757.

**Kim, J. B., Wright, H. M., Wright, M., and Spiegelman, B. M.** (1998). SREBP1 activates PPAR $\gamma$  through the production of endogenous ligand. *Proc. Natl. Acad. Sci. U S A* **95**,4333-4337.

**Kim, S., You, S., and Hwang, D.** (2011). Aminoacyl-tRNA synthetases and tumorigenesis: more than housekeeping. *Nat. Rev. Cancer* **11**,708-718.

**Koppen, A., and Kalkhoven, E.** (2010). Brown vs white adipocytes: the PPAR $\gamma$  coregulator story. *FEBS Lett.* **584**,3250-3259.

**Kubo, M., Ijichi, N., Ikeda, K., Horie-Inoue, K., Takeda, S., and Inoue, S.** (2009). Modulation of adipogenesis-related gene expression by estrogen-related

receptor gamma during adipocytic differentiation. *Biochim Biophys Acta*. **1789**,71-77.

**Lee, S. W., Cho, B. H., Park, S. G., and Kim, S.** (2004). Aminoacyl-tRNA synthetase complexes: beyond translation. *J. Cell Sci.* **117**,3725-3734.

**Lefterova, M. I., Zhang, Y., Steger, D. J., D., Zhuo, D., Stoeckert, C. J. Jr., and Liu, X. S.,** (2008). PPARgamma and C/EBP factors orchestrate adipocyte biology via adjacent binding on a genome-wide scale. *Genes Dev.* **22**, 2941-2952.

**Marchildon, F., St-Louis, C., Akter, R., Roodman, V., and Wiper-Bergeron, N. L.** (2010). Transcription factor Smad3 is required for the inhibition of adipogenesis by retinoic acid. *J. Biol. Chem.* **285**,13274-13284.

**Méndez-Sánchez, N., Chavez-Tapia, N. C., Zamora-Valdés, D., and Uribe, M.** (2006). Adiponectin, structure, function and pathophysiological implications in non-alcoholic fatty liver disease. *Mini. Rev. Med. Chem.* **6**,651-656.

**Mirande, M., Gache, Y., Le Corre, D., and Waller, J. P.** (1982). Seven mammalian aminoacyl-tRNA synthetases co-purified as high molecular weight entities are associated within the same complex. *EMBO J.* **1**,733-736.

**Norcum, M. T.** (1989). Isolation and electron microscopic characterization of the high molecular mass aminoacyl-tRNA synthetase complex from murine erythroleukemia cells. *J. Biol. Chem.* **264**,15043-15051.

**Ntambi, J. M., and Young-Cheul, K.** (2000). Adipocyte differentiation and gene expression. *J. Nutr.* **130**,3122S-3126S.

**Park, H., Park, S. G., Kim, J., Ko, Y. G., and Kim, S.** (2002a). Signaling pathways for TNF production induced by human aminoacyl-tRNA synthetase-associating factor, p43. *Cytokine* **20**,148-153.

**Park, S. G., Kang, Y. S., Ahn, Y. H., Lee, S. H., Kim, K. R., Kim, K. W., Koh, G. Y., Ko, Y. G., and Kim, S.** (2002b). Dose-dependent biphasic activity of tRNA synthetase-associating factor, p43, in angiogenesis. *J. Biol. Chem.* **277**,45243-45248.

**Park, S. G., Kang, Y. S., Kim, J. Y., Lee, C. S., Ko, Y. G., Lee, W. J., Lee, K. U., Yeom, Y. I., and Kim, S.** (2006). Hormonal activity of AIMP1/p43 for glucose homeostasis. *Proc. Natl. Acad. Sci. U S A.* **103**,14913-14918.

**Park, S. G., Jung, K. H., Lee, J. S., Jo, Y. J., Motegi, H., Kim, S., and Shiba, K.** (1999). Precursor of pro-apoptotic cytokine modulates aminoacylation activity of tRNA synthetase. *J. Biol. Chem.* **274**,16673-16676.

**Park, S. G., Schimmel, P., and Kim, S.** (2008). Aminoacyl tRNA synthetases and their connections to disease. *Proc. Natl. Acad. Sci. U S A.* **105**,11043-11049.

**Park, S. G., Shin, H., Shin, Y. K., Lee, Y., Choi, E. C., Park, B. J., and Kim, S.** (2005). The novel cytokine p43 stimulates dermal fibroblast proliferation and wound repair. *Am. J. Pathol.* **166**,387-398.

**Picard, F., Kurtev, M., Chung, N., Topark-Ngarm, A., Senawong, T., Machado De Oliveira, R., Leid, M., McBurney, M. W., and Guarente, L.** (2004). Sirt1 promotes fat mobilization in white adipocytes by repressing PPAR-gamma. *Nature* **429**,771-776.

**Quevillon, S., Agou, F., Robinson, J. C., and Mirande, M.** (1997). The p43 component of the mammalian multi-synthetase complex is likely to be the precursor of the endothelial monocyte-activating polypeptide II cytokine. *J. Biol. Chem.* **272**,32573-32579.

**Quevillon, S., and Mirande, M.** (1996). The p18 component of the multisynthetase complex shares a protein motif with the beta and gamma subunits of eukaryotic elongation factor 1. *FEBS Lett.* **395**,63-67.

**Quevillon, S., Robinson, J-C., Berthonneau, E., Siatecka, M., and Mirande, M.** (1999). Macromolecular assemblage of aminoacyl-tRNA synthetases: identification of protein-protein interactions and characterization of a core protein. *J. Mol. Biol.* **285**,183-195.

**Rosen, E. D., and Spiegelman, B. M.** (2006). Adipocytes as regulators of energy balance and glucose homeostasis. *Nature* **444**,847-853.

**Rosen, E. D., Sarraf, P., Troy, A. E., Bradwin, G., Moore, K., Milstone, D. S., Spiegelman, B. M., and Mortensen, R. M.** (1999). PPAR-gamma is required for the differentiation of adipose tissue in vivo and in vitro. *Mol. Cell* **4**,611-617.

- Rosen, E. D., Walkey, C. J., Puigserver, P., Spiegelman, B. M.** (2000). Transcriptional regulation of adipogenesis. *Genes Dev.* **14**,1293-1307.
- Spiegelman, B. M.** (1998). PPAR-gamma: adipogenic regulator and thiazolidinedione receptor. *Diabetes* **47**,507-514.
- Tang, Q. Q., Otto, T. C., Lane, M. D.,** (2003). Mitotic clonal expansion: a synchronous process required for adipogenesis. *Proc Natl Acad Sci U S A.* **100**,44-49.
- Tontonoz, P., Hu, E., and Spiegelman, B. M.** (1994). Stimulation of adipogenesis in fibroblasts by PPAR gamma 2, a lipid-activated transcription factor. *Cell* **79**,1147-1156.
- Tontonoz, P., and Spiegelman, B. M.** (2008). Fat and beyond: the diverse biology of PPARgamma. *Annu. Rev. Biochem.* **77**,289-312.
- Trayhurn P., and Beattie J. H.** (2001). Physiological role of adipose tissue: white adipose tissue as an endocrine and secretory organ. *Proc. Nutr. Soc.* **60**,329-339.
- Wang, F., and Tong, Q.** (2009). SIRT2 suppresses adipocyte differentiation by deacetylating FOXO1 and enhancing FOXO1's repressive interaction with PPARgamma. *Mol. Biol. Cell.* **20**,801-808.
- Wu, Z., Xie, Y., Morrison, R. F., Bucher, N. L., and Farmer, S. R.** (1998). PPAR $\gamma$  induces the insulin-dependent glucose transporter GLUT4 in the absence of C/EBP $\alpha$  during the conversion of 3T3 fibroblasts into adipocytes. *J. Clin. Invest.* **101**,22-32.
- Yamada, T., Katagiri, H., Ishigaki, Y., Ogihara, T., Imai, J., Uno, K., Hasegawa,**

**Y., Gao, J., Ishihara, H., Nijima, A., Mano, H., Aburatani, H., Asano, T., Oka, Y.** (2006). Signals from intra-abdominal fat modulate insulin and leptin sensitivity through different mechanisms: neuronal involvement in food-intake regulation. *Cell Metab.* **3**,223-229.

**Yu, C., Markan, K., Temple, K. A., Deplewski, D., Brady, M. J., and Cohen, R. N.** (2005). Nuclear receptor corepressors NCoR and SMRT decrease peroxisome proliferator activated receptor gamma transcriptional activity and repress 3T3L1 adipogenesis. *J. Biol. Chem.* **280**,13600-13605.

**Yu, S., Matsusue, K., Kashireddy, P., Cao, W. Q., Yeldandi, V., Yeldandi, A. V., Rao, M. S., Gonzalez, F. J., and Reddy, J. K.** (2003). Adipocyte-specific gene expression and adipogenic steatosis in the mouse liver due to peroxisome proliferator-activated receptor gamma1 (PPARgamma1) overexpression. *J. Biol. Chem.* **278**,498-505.

**Zamir, I., Zhang, J., and Lazar, M. A.** (1997). Stoichiometric and steric principles governing repression by nuclear hormone receptors. *Genes Dev.* **11**, 835-846.

**Zebisch, K., Voigt, V., Wabitsch, M., Brandsch, M.** (2012). Protocol for effective differentiation of 3T3-L1 cells to adipocytes. *Anal Biochem.* **425**,88-90.

**Zhang, K., Guo, W., Yang, Y., and Wu, J.** (2011). JAK2/STAT3 pathway is involved in the early stage of adipogenesis through regulating C/EBP $\beta$  transcription. *J. Cell Biochem.* **112**,488-497.

## Figure legends

### **Fig. 1. Expression of genes encoding aminoacyl-tRNA synthetases (ARSs) and aminoacyl-tRNA synthetase-interacting multifunctional proteins (AIMPs) during the differentiation of 3T3-L1 preadipocytes.**

**A.** A heat map of mRNA expression in 3T3-L1 cells during adipogenesis. 3T3-L1 preadipocytes were differentiated, and harvested every 2 days. The initial day of differentiation was designed day 0 and the color, every other day, is shown as a relative percentage. Quantification of mRNA expression is represented by a heat map in a 10% scale, from green to red. **B.** Total RNA was extracted from cell lysates and quantitative RT-PCR was performed using specific primers. As a control, *GAPDH* mRNA levels were also quantified from the same RNA samples by RT-PCR. The level of each gene transcript was normalized to that of *GAPDH*. The data shown are representative of three independent experiments. **C.** 3T3-L1 preadipocytes were differentiated, harvested every 2 days, lysed with lysis buffer, and the lysate proteins then separated by SDS-PAGE, and immunoblotted using the indicated antibodies. The data shown are representative of three independent experiments. **D.** Total RNA was extracted from embryos and postnatal days 0, 2, 4 of C57BL/6 mice and quantitative RT-PCR was performed using specific primers. As a control, *GAPDH* mRNA levels were also quantified from the same RNA samples by RT-PCR. The level of each gene transcript was normalized to that of *GAPDH*. The data shown are representative of three independent experiments.

**Fig. 2. AIMP1 translocates to the nucleus in 3T3-L1 adipocytes.**

**A.** Immunofluorescence assays, using anti-AIMP1 antibodies (green), were performed in 3T3-L1 preadipocytes and 3T3-L1 adipocytes. Propidium iodide (PI) was used as a nuclear stain. **B.** The cytosol and nucleus of 3T3-L1 adipocytes were fractionated at the indicated days, as described in Materials and Methods. Cell lysates were separated by SDS-PAGE, and immunoblotted using antibodies against AIMP1, YY1 (a nuclear marker), and HSP90 (a cytoplasmic marker). **C.** 3T3-L1 preadipocytes were transfected with GFP-AIMP1 (full length), GFP-C-terminal truncated mutant (a.a. 1-146), or GFP-N-terminal truncated mutant (a.a. 147-312), respectively. Images were visualized with fluorescence microscope. **D.** AIMP1 primary sequence showing candidate nuclear targeting motif. **E.** The cytoplasm and nucleus were fractionated after the transfection with Myc-AIMP1 WT or Myc-AIMP1 mutant (KKK267-269AAA), as described in Materials and Methods. Cell lysates were separated by SDS-PAGE, and immunoblotted using antibodies against Myc, YY1 (a nuclear marker), and HSP90 (a cytoplasmic marker). **F.** 3T3-L1 preadipocytes were differentiated; thereafter, the culture media was harvested at the indicated days. The amount of secreted adiponectin and AIMP1 was quantified using specific ELISA kits. The data shown are representative of three independent experiments, and are shown as mean and S.D. (error bars). n = 3.

**Fig. 3. Silencing of AIMP1 promotes adipogenesis.**

**A.**  $AIMP1^{+/+}$  and  $AIMP1^{-/-}$  MEFs were differentiated as described in Materials and Methods. At day 8 after differentiation, total RNA was extracted from  $AIMP1^{+/+}$  and  $AIMP1^{-/-}$  MEFs. RT-PCR was performed using specific primers. **B.** 3T3-L1 preadipocytes were transfected with siRNA directed against *AIMP1* or with a control siRNA, differentiated, and harvested at the indicated day. RT-PCR was performed using specific primers. **C.**  $AIMP1^{+/+}$  and  $AIMP1^{-/-}$  MEFs were differentiated and stained with Oil-red O staining solution. High-magnification images are shown in the bottom panels. **D.** 3T3-L1 preadipocytes were transfected with siRNA directed against or with a control siRNA, differentiated, and stained with Oil-red O staining solution. High-magnification images are shown in the bottom panels. **E.** TG contents were measured in  $AIMP1^{+/+}$  and  $AIMP1^{-/-}$  MEFs during differentiation. ( $p = 0.0006$ , at day 12). **F.** 3T3-L1 preadipocytes were transfected with siRNA directed against *AIMP1* or with a control siRNA. During differentiation, TG contents were measured at the indicated days. ( $p = 0.0041$ , at day 8). **G.**  $AIMP1^{+/+}$  and  $AIMP1^{-/-}$  MEFs were differentiated, harvested at the indicated days, and lysates immunoblotted using the indicated antibodies. **H.** 3T3-L1 preadipocytes were transfected with siRNA directed against *AIMP1* or with a control siRNA, differentiated, and lysates immunoblotted using the indicated antibodies. The data shown are representative of three independent experiments, and are represented as mean and S.D. ( $n = 3$ ).

**Fig. 4. Overexpression of AIMP1 delays adipogenesis.**

**A.** AIMP1-inducible cell lines, which were cultured in the presence or absence of tetracycline (tet), were differentiated, harvested at days 0, 4, or 8, and immunoblotted using the indicated antibodies. **B.** AIMP1-inducible cell lines were differentiated, and then stained with Oil-red O solution. High-magnification images are shown in the bottom panels. **C.** TG contents in AIMP1-inducible cell lines that had been cultured in the presence or absence of tet, were measured during differentiation. ( $p = 0.0006$  at day 4,  $p < 0.0001$  at day 8). **D.** 3T3-L1 preadipocytes were infected with AdV-LacZ or AdV-AIMP1, harvested at 0, 4, 8, 12 days after differentiation, and immunoblotted using the indicated antibodies. **E.** 3T3-L1 preadipocytes were infected with AdV-LacZ or AdV-AIMP1. After differentiation, 3T3-L1 adipocytes were stained with Oil-red O solution. High-magnification images are shown in the bottom panels. **F.** 3T3-L1 preadipocytes were infected with AdV-LacZ or AdV-AIMP1. After differentiation, TG contents were measured. Data are shown as mean and S.D. ( $n = 3$ ).  $p = 0.0037$  at day 4,  $p = 0.0014$  at day 8,  $p < 0.01$  at day 12.

**Fig. 5. The effects of AIMP1 on adipogenesis *in vivo*.**

The mouse fat pad was injected with AdV-LacZ or AIMP1 as described in Materials and Methods. **A.** The white adipocyte (WAT), liver, and muscle were extracted from mice, lysed with lysis buffer, separated by SDS-PAGE and immunoblotted with the indicated antibodies. Body weight (B), blood AIMP1 levels (C), serum TNF $\alpha$  levels

(D), serum adiponectin levels (E) serum TG levels (F), serum NEFA levels (G), and serum insulin levels (H) of LacZ mice and AIMP1 mice on day 3 after adenoviral administration. (I). Glucose-tolerance test was performed on day 3. Data are presented as means and S.D. (n = 6 per group). \* $p < 0.05$  by unpaired t-test.

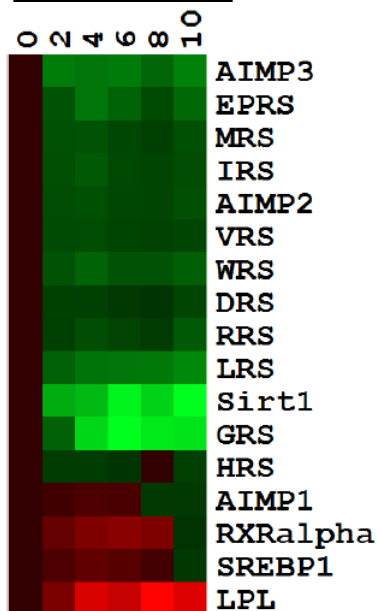
**Fig. 6. AIMP1 regulates PPAR $\gamma$  transcriptional activity through a direct binding with PPAR $\gamma$ .**

**A.** HEK293 cells were transfected with the indicated plasmids, including those expressing PPAR $\gamma$  and AIMP1 (0, 1, 2, 5 $\mu$ g), and reporter plasmids, such as the PPAR $\gamma$  response element-luciferase construct (PPRE-tk-Luc). Cells were treated with the PPAR $\gamma$  agonist rosiglitazone (1  $\mu$ M, 24h) and harvested for the luciferase assays. The luciferase activity of PPAR $\gamma$  was measured in the presence or absence of rosiglitazone. Luciferase activity was normalized to  $\beta$ -gal activity. **B.** HEK293 cells were transfected with the indicated plasmids, including PPAR $\gamma$ , AIMP1, or RXR $\alpha$ . After transfection, cells were harvested for the luciferase assays. Luciferase activity was normalized to  $\beta$ -gal activity. **C.** Differentiated 3T3-L1 adipocytes were harvested, lysed, and immunoprecipitated using AIMP1 antibodies or control IgG. AIMP1 co-immunoprecipitated with PPAR $\gamma$ . **D.** 293T cells that had been transfected with myc-AIMP1 and either GFP-PPAR $\gamma$  or PPAR $\alpha$  were harvested, lysed, and immunoprecipitated using an anti-myc antibody or IgG as a control. The immunoprecipitates were immunoblotted with the indicated antibodies. **E.**

Schematic diagram and individual fragments of PPAR $\gamma$  used in this study (upper panel). HEK293 cells were transfected with myc-AIMP1 and GFP-PPAR $\gamma$  constructs. myc-AIMP1 was co-immunoprecipitated with particular GFP-PPAR $\gamma$  constructs, such as PPAR $\gamma$ -D, and PPAR $\gamma$ -DL. **F.** Cell lysates from 3T3-L1 cells treated with DMSO, GW9662 (1  $\mu$ M, 24 h), or rosiglitazone (1  $\mu$ M, 24 h) were mixed with GST-AIMP1 (full length) and affinity precipitated using glutathione-sepharose beads. Co-precipitation of PPAR $\gamma$  with GST-AIMP1 was assessed by immunoblotting with an anti-PPAR $\gamma$  antibody. **G.** The endogenous PPAR $\gamma$  in nuclear extracts interacted with the PPAR $\gamma$ -response element (PPRE). Purified AIMP1 was added in the indicated dose and inhibited the binding of PPAR $\gamma$  in a dose-dependent manner. Competitor was used as a positive control. **H.** 3T3-L1 adipocytes were transfected with either control (EV) or AIMP1. Immuno-complexes were precipitated with control IgG or PPAR $\gamma$  antibodies and PCR was performed using primers specific for the genes encoding aP2, LPL, and Gyl. Data are presented as means and S.D.

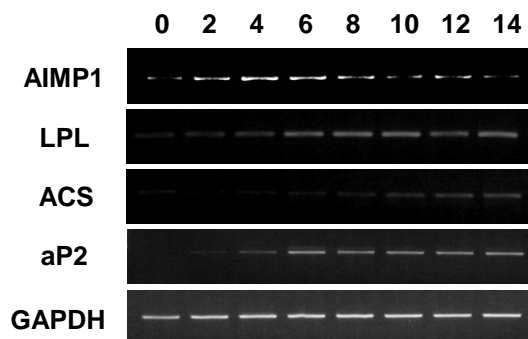
**A**

Time after differentiation (days)



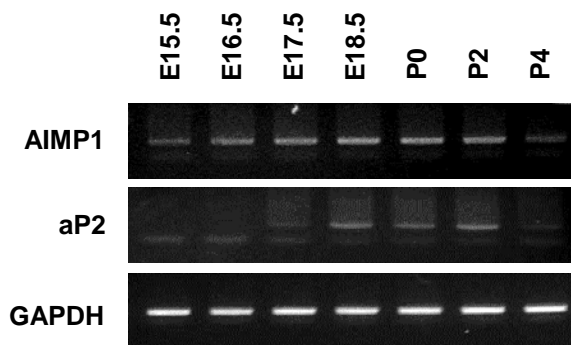
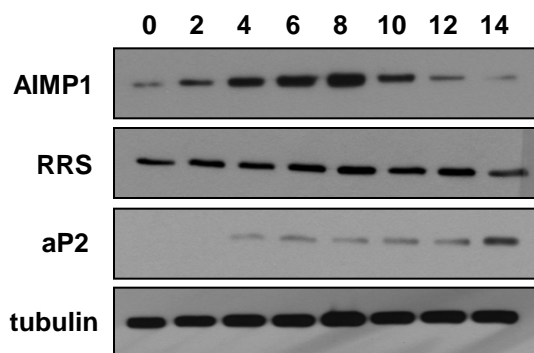
**B**

Time after differentiation (days)

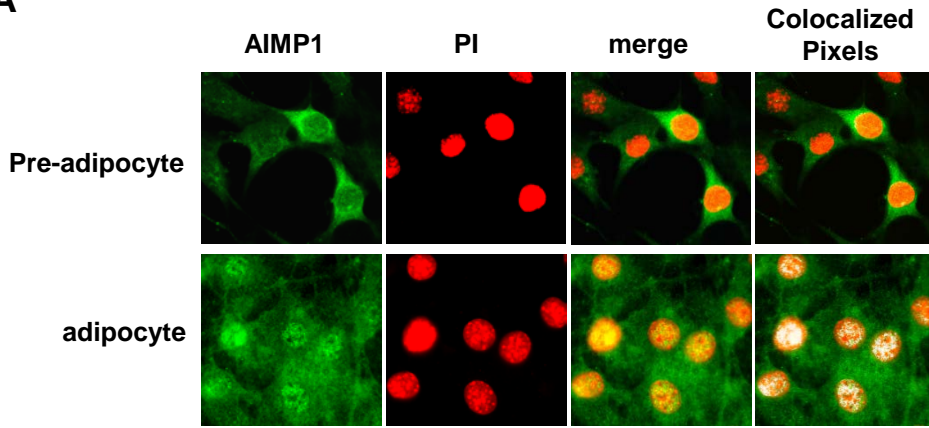


**D**

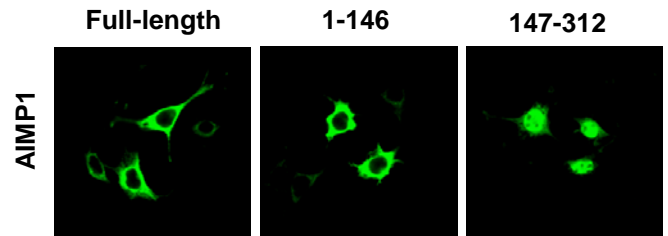
Time after differentiation (days)



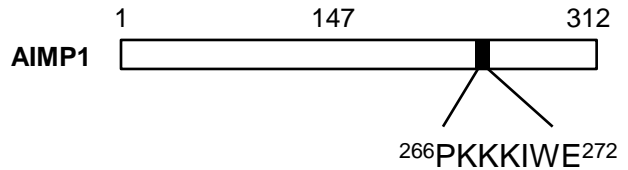
**A**



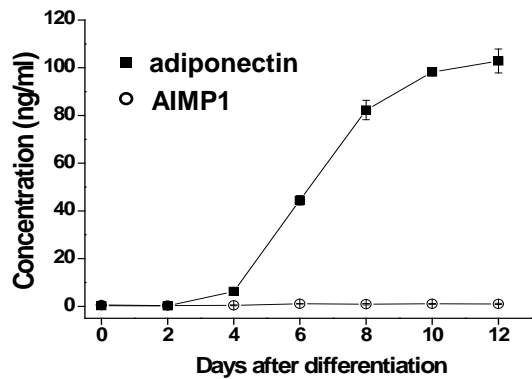
**C**



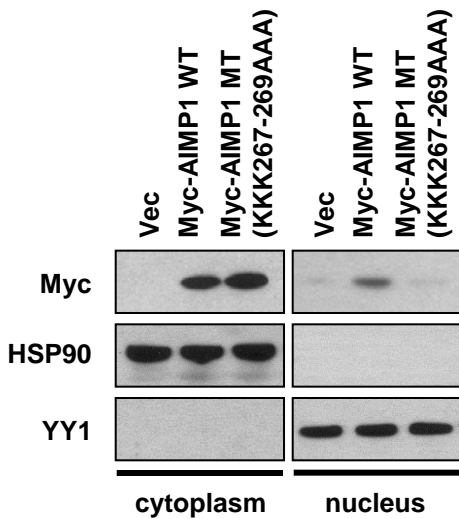
**D**

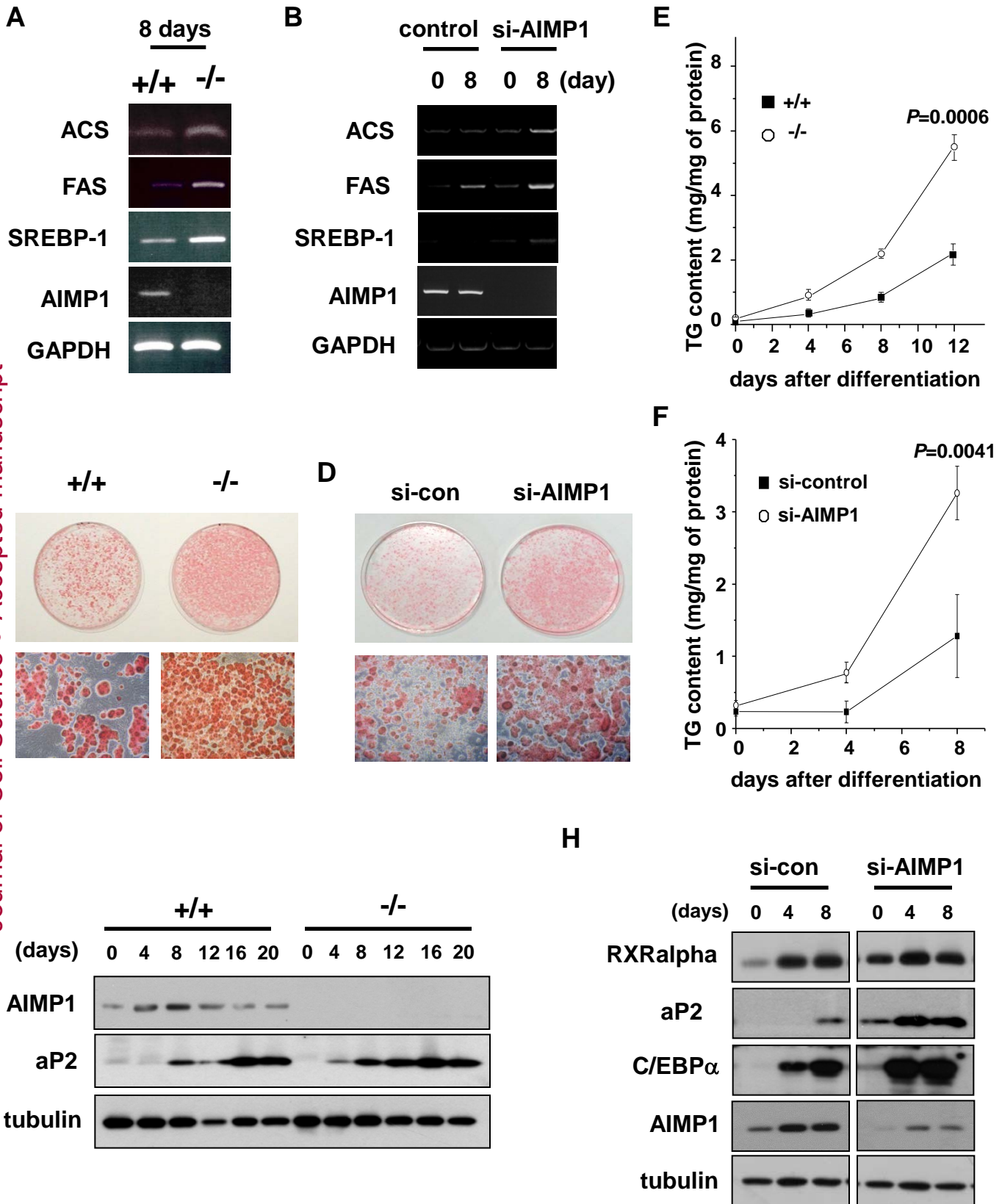


**F**

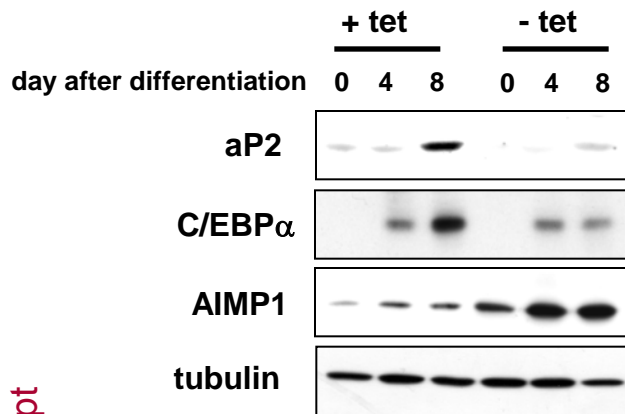


**E**

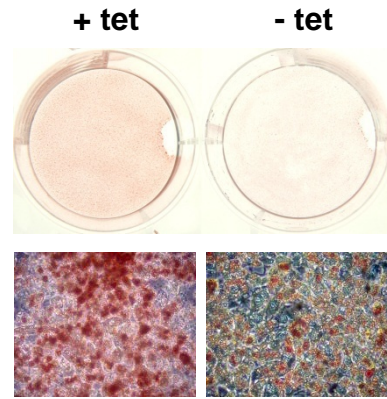




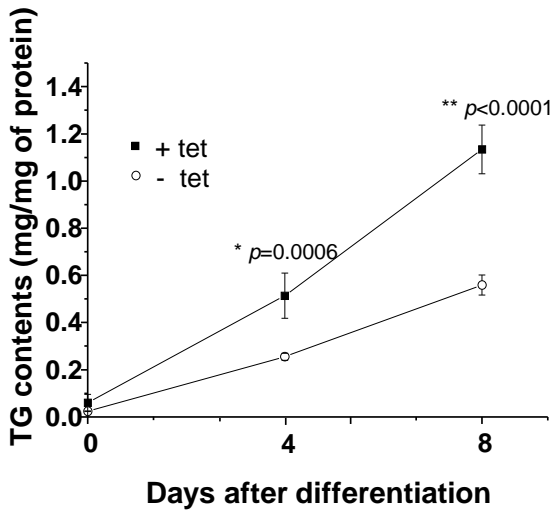
**A**



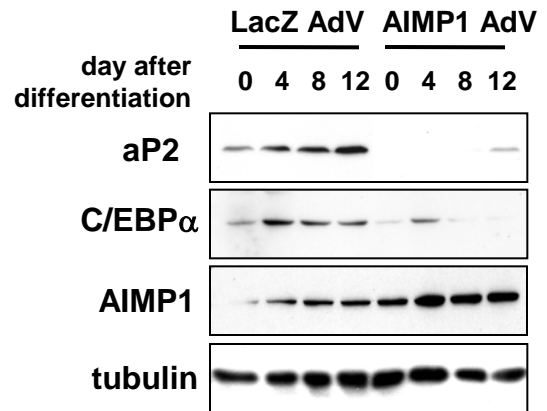
**B**



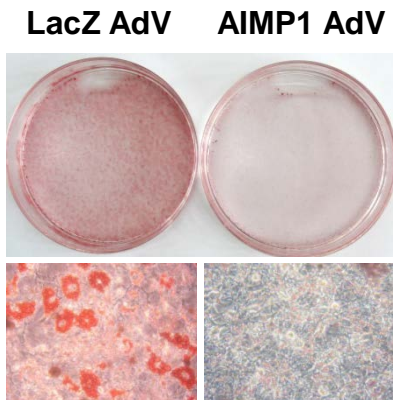
**C**



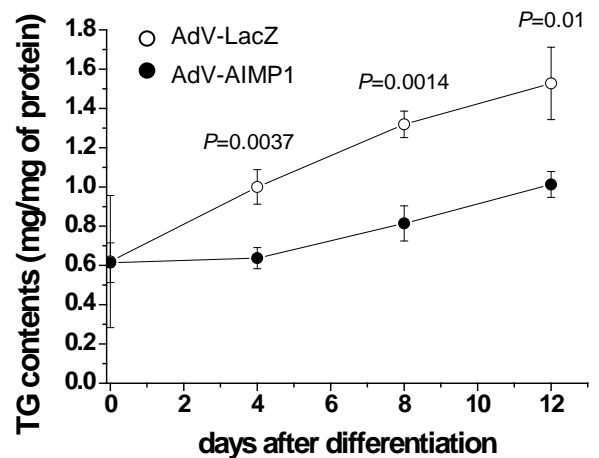
**D**



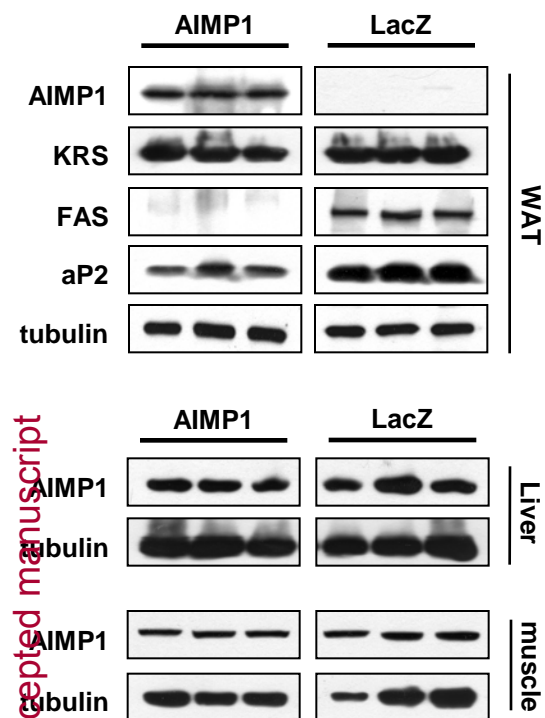
**E**



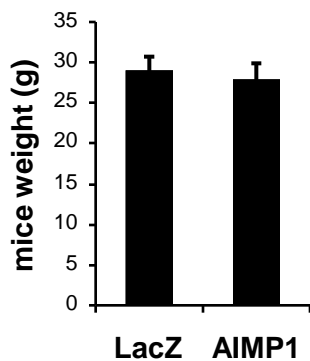
**F**



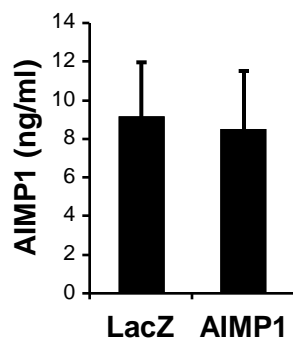
A



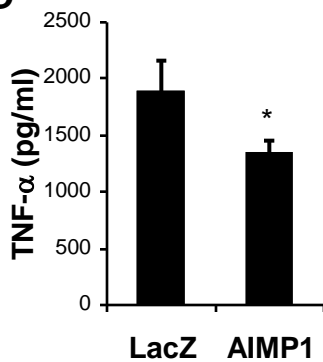
B



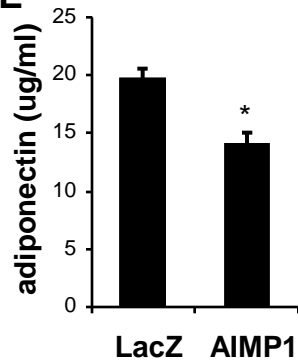
C



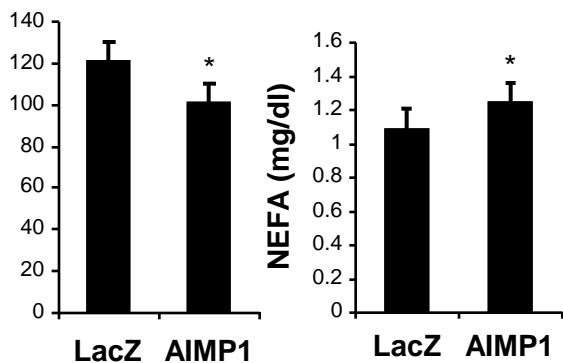
D



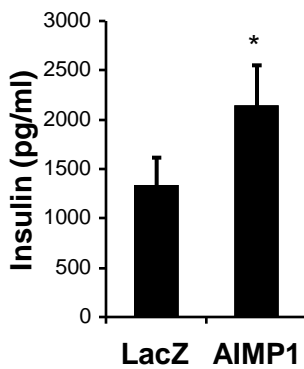
E



G



H



I

